Brief Report

Human locomotion-control brain networks detected with independent component analysis

Pengxu Wei[1,2], Tong Zou[2], Zeping Lv[1,2], Yubo Fan[1,2,*]

[1] *Key Laboratory of Biomechanics and Mechanobiology (Beihang University), Ministry of Education, Beijing Advanced Innovation Center for Biomedical Engineering, School of Biological Science and Medical Engineering, Beihang University, 100083 Beijing, China*

[2] *Beijing Key Laboratory of Rehabilitation Technical Aids for Old-Age Disability, Key Laboratory of Neuro-functional Information and Rehabilitation Engineering of the Ministry of Civil Affairs, National Research Center for Rehabilitation Technical Aids, 100176 Beijing, China*

*Correspondence: yubofan@buaa.edu.cn (Yubo Fan)

DOI:10.31083/j.jin2003074

Submitted: 4 July 2021 Revised: 10 August 2021 Accepted: 24 August 2021 Published: 30 September 2021

Walking is a fundamental movement skill in humans. However, how the brain controls walking is not fully understood. In this functional magnetic resonance imaging study, the rhythmic, bilaterally alternating ankle movements were used as paradigm to simulate walking. In addition to the resting state, several motor tasks with different speeds were tested. Independent component analysis was performed to detect four components shared by all task conditions and the resting state. According to the distributed brain regions, these independent components were the cerebellum, primary auditory cortex–secondary somatosensory cortex–inferior parietal cortex–presupplementary motor area, medial primary sensorimotor cortex–supplementary area–premotor cortex–superior parietal lobule, and lateral primary somatosensory cortex–superior parietal lobule–dorsal premotor cortex networks, which coordinated limb movements, controlled the rhythm, differentiated speed, and performed a function as a basic actor network, respectively. These brain networks may be used as biomarkers of the neural control of normal human walking and as targets for neural modulation to improve different aspects of walking, such as rhythm and speed.

Keywords

Human walking; Motor control; Brain network; fMRI; Independent component analysis

1. Introduction

Walking is a fundamental movement skill in humans. To date, how the brain controls walking in normal adults is still not fully understood. Several functional magnetic resonance imaging (fMRI) studies applied various motor tasks to simulate walking or components of walking, including unilateral leg movements [1–11], alternating bilateral leg movements [12, 13], leg movements with the foot pedal [5, 9–11] providing force feedback or without resistance [12], and imagined foot movements [14] or walking [15–18]. These studies found that several brain regions, including the inferior parietal cortex (IPC), primary motor cortex (M1), premotor cortex (PreM, including dorsal [PMd] and ventral parts [PMv]), presupplementary motor area (preSMA), supplementary motor area (SMA), primary and secondary somatosensory cortices (S1 and S2), superior parietal lobule (SPL), and many other areas, such as the primary auditory cortex (PAC), participate in locomotion control during audio-cued conditions.

In animal experiments investigating locomotion-control mechanisms, rhythmic muscle activity and left–right alternating leg movements are considered as core factors of locomotion or walking [19]. This criterion is also adopted in a human study exploring the effects of several drugs on restoring locomotion capabilities in patients suffering a motor-complete spinal cord injury. The study found that the electromyography activity of four muscles of each leg presents locomotion-like features, that is, rhythmic, bilaterally alternating muscle activities in the lower limbs [20]. Here, we also adopt motor tasks consisting of these components as core feature to simulate human walking. A normal subject can change the speed/frequency of steps to meet the needs of the context. Thus, several motor tasks with core components but different frequencies are also applied to set up corresponding relationships between the designed tasks and the different types of walking in real scenes.

Most of the abovementioned fMRI studies applied a model-based analysis, which predicts blood oxygen level-dependent (BOLD) responses evoked by motor tasks with the hemodynamic response function (HRF) model. However, a transient response at the onset of a stimulus [21] or adaptation-related brain activities [22] may not be captured by the HRF model. As a data-driven approach, the independent component analysis (ICA) can detect distributed brain networks with different BOLD signal time courses without making a specific modeling assumption, such as a canonical HRF model, and identify motion-related noise from resting-state and task fMRI data [23].

The patterns of brain organization during task and resting states share some similarities [24]. However, different features may also be present [25]. ICA can separate independent sources from task- and resting-based fMRI data, and the

Journal of Integrative Neuroscience

spatial and temporal features of these independent components (ICs) from different states can be compared.

In this study, the ICA is used to separate independent sources from a set of fMRI data consisting of motor tasks to simulate walking. Several brain networks are expected to be detected to control the core components of human walking and identify their functions in different walking status.

2. Materials and methods

2.1 Subjects, tasks, and MRI data acquisition

MRI data were collected from 20 healthy right-handed subjects (10 males/females, 24.5 $\pm$ 2.16 years).

The fMRI experiment contained six successive sessions for every volunteer. The first session had a duration of 480 s, and resting-state fMRI data were collected. The second session tested a self-paced, free-speed walking task to simulate a usual walk without pressure following an audio alert "alternating left and right sides in a free speed and keeping a constant speed" repeated five times for 30 s. Subjects were instructed to perform ankle dorsiflexion and plantarflexion alternately and repeatedly to simulate rhythmic, bilaterally alternating muscle activities in the lower limbs during walking. The following four sessions tested ankle movements at 0.5, 1, and 2 Hz frequencies or a changing speed in a counterbalanced order for every four subjects. Subjects paced the movements following the audio alert "left–right–left–right…" at preset frequencies. The 0.5, 1, and 2 Hz conditions consisted of 15, 30, and 60 audio alerts, respectively, during a task block. The audio alert had a fixed order in every task block of changing-speed conditions: 4 audio alerts with 1 Hz, 6 alerts with 1.5 Hz, 8 alerts with 2 Hz, 6 alerts with 1.5 Hz, 8 alerts with 2 Hz, 8 alerts with 1.5 Hz, and 4 alerts with 1 Hz with an average frequency of 1.47 Hz.

The following four sessions were counterbalanced for every four subjects in the order of arrival to the MRI room.

During fMRI scanning, each subject was instructed to close his/her eyes but remain awake while lying in a supine position with a pad under the knees to support the thighs to relax the spine and prevent motion from transferring to the head during ankle movements [10].

A monitoring system displayed the real-time amplitude of translational head motions of the subject during MR scanning. Data scanning was restarted if head movements surpassed 1 mm in the *x*-, *y*-, or *z*-axis.

T2* images were collected using the Siemens Prisma 3T MRI (Siemens Healthineers Ltd., Germany) system (time of repetition [TR], 2000 ms; time of echo [TE], 30 ms; flip angle, 90°; and voxel size, 2.0 $\times$ 2.0 $\times$ 2.0 mm) consisting of 64 interleaved axial slices with 0.2 mm gaps between slices. The 3D MPRAGE sequence was used to acquire T1-weighted images (TR, 2530 ms; TE, 2.98 ms; flip angle, 7°; inversion time, 1100 ms; and voxel size, 0.5 $\times$ 0.5 $\times$ 1.0 mm). Field mapping images were also collected (TR, 635 ms; TE, 4.92 and 7.38 ms; flip angle, 60°; and voxel size 2.0 $\times$ 2.0 $\times$ 2.0 mm).

MRI data were obtained from a previous study [26], which focused on brainstem and brain activations by using the model-based approach and investigated the region of interest-based functional connectivity measured with Pearson correlation coefficients.

Data and the informed consent of all participants were obtained. The institutional review board of the National Research Center for Rehabilitation Technical Aids approved the protocol (code: 2018YFC2001401).

2.2 Data analysis

The SPM software (SPM12, Wellcome Centre for Human Neuroimaging, University College London, https://www.fil.ion.ucl.ac.uk/spm/software/spm12) was used for temporal and spatial preprocessing. Differences in slice acquisition times of functional images were corrected first. The FieldMap Toolbox was applied while performing realignment and unwarped simultaneously to correct head motion and geometric distortion. T2* and T1 images were coregistered and normalized to the standard MNI space as introduced in [27].

ICA was performed using the GIFT4.0b (http://mialab.mrn.org/software/gift/index.html). The number of ICs from each condition was estimated with the minimum description length criteria [28]. The Infomax algorithm [29] was repeated 10 times with the ICASSO [30] to separate ICs from the fMRI data set of each condition. The one-sample *t* test was used to acquire the contrast images and *t* map of each component (against the null of zero task-related change either positive or negative, i.e., a two-sided test) [31]. The spatial map of each component was then acquired using the SPM software at a threshold of $p < 0.001$ with a cluster extent of more than 10 contiguous voxels.

Motion artifacts were identified in accordance with previous studies [32–35] if the main part of a component was located on large vessels (e.g., superior sagittal or transverse sinus), margins of the brain (displaying ring-like shapes), or regions full of cerebrospinal fluid, such as that surrounding the brainstem.

Task-evoked ICs were identified if the Pearson correlation coefficient $\geq$0.3 when performing "temporal sorting" function for task fMRI data sets with the GIFT software. ICs with correlation coefficient <0.3 might present a spatial pattern similar to that of the default mode network, which is found to be uncoupled from task waveform.

Spatial correlation coefficients between each IC map of each condition and all other IC maps of the remaining conditions were calculated to identify task-evoked components that commonly appeared in all conditions. For a component, strong and positive correlation values indicated that the spatial map of this component was stable across all conditions, and the brain regions in the spatial map of this component constituted a distributed brain network.

3. Results

3.1 Task-related components that commonly appeared in all conditions

The estimated numbers of ICs in each condition were 25 (0.5 Hz), 26 (1 Hz), 26 (2 Hz), 25 (changing-speed condition), 26 (free-speed condition), and 27 (resting-state condition). Three task-related components that commonly appeared in all conditions presented positive correlation >0.3 for each task condition. On the basis of their spatial maps, these ICs were named as cerebellum, PAC-S2-IPC-preSMA, and medial M1S1-SMA-PreM-SPL networks. In addition, one component presented negative correlations with the task time course in 0.5 and 1 Hz conditions but positive correlations with the task time course in the 2 Hz, changing-speed (average frequency = 1.47 Hz), and free-speed (average frequency = 1.46 $\pm$ 0.67 Hz) conditions. This component was also detected in the resting state and named the lateral S1-SPL-PMd network on the basis of its spatial map.

The common spatial map of each of the four components across all conditions (Fig. 1) was determined using the inclusive masking function in the SPM software at primary thresholds of $p < 0.001$ and $p < 0.05$ family-wise error corrected cluster extent provided by the SPM toolbox for the whole search volume.

3.2 Pairwise spatial correlation values among different conditions

The cerebellum network was distributed in the cerebellum (from z = –55 to z = –10 in Fig. 1). The PAC-S2-IPC-preSMA network (**Supplementary Figs. 1,2**) was mainly distributed in the PAC and S2. Some parts of the network were distributed in the IPC and preSMA. The PAC is located at Heschl's gyrus, including cytoarchitectonic subdivisions TE 1.0, 1.1, and 1.2 [36] and at the medial part of the temporal pole lateral to the posterior insula [37].

The lateral S1-SPL-PMd network (**Supplementary Figs. 3,4**) was mainly distributed in the parietal cortex (lateral parts of S1 and SPL). Some parts of the network were distributed in the PMd. The extensions of preSMA, SMA, and PMd were determined using a meta-analysis [38].

The medial M1S1-SMA-PreM-SPL network was mainly distributed in the medial parts of the primary sensorimotor cortex (M1 and S1). This component also covered bilateral SMA, PreM, and SPL (**Supplementary Figs. 5,6**). The scopes of these brain regions except that of SMA were determined using the SPM Anatomy toolbox.

For each of the four components (networks), the pairwise spatial correlation values among different conditions are shown in Table 1. Under most conditions, the medial M1S1-SMA-PreM-SPL network presented the lowest correlation value, ranging from 0.30 to 0.38 between the resting-state and other conditions. However, the pairwise correlation values of the components between the task conditions were not less than 0.54. These results indicated that this network exhibited much more variations between resting-state and task states than between different task conditions. As shown in **Supplementary Fig. 7**, the network covered lateral parts of M1 and S1 during the resting state and medial parts of these brain regions during task conditions.

Correlation values were ranked in descending order in each row. The cerebellum network always presented the highest correlation value, that is, the most consistent spatial maps across all conditions. Under most conditions, the lateral S1-SPL-PMd network presented the second highest correlation value, whereas the medial M1S1-SMA-PreM-SPL network presented the lowest correlation value.

4. Discussion

Four task-related ICs, namely, cerebellum, PAC-S2-IPC-preSMA, medial M1S1-SMA-PreM-SPL, and lateral S1-SPL-PMd networks, are found. These brain networks can also be detected during the resting state. Findings reveal the interaction among a number of brain regions during the state of a simulated walking task. The four brain networks work together to control the simulated walking patterns, i.e., rhythmic, bilaterally alternating ankle movements.

4.1 Cerebellum network

The cerebellum network covers most parts of the cerebellum and exhibits the highest level of consistency across all conditions (Table 1). These findings suggest that this component plays a fundamental role in walking control. Compared with simple limb movements, the cerebellum is more likely to participate in modulating complicated movements [39]. Additionally, the cerebellum is a place to modulate movements with somatosensory inputs [40]. The motor tasks applied in this study are bilaterally involved alternating ankle dorsiflexion and plantarflexion, which are more complex than unilateral ankle movements and require more somatosensory information for feedforward and feedback controls. Therefore, this component covers extensive areas of the cerebellum.

The cerebellum is responsible for the coordination of movements, especially skilled voluntary motor tasks. Cerebellar lesions lead to incoordination (ataxia) of volitional movement and gait disorders [41]. Therefore, the bilaterally alternating ankle dorsiflexion–plantarflexion movements depend on cerebellar functions.

4.2 Rhythm-control network

The PAC-S2-IPC-preSMA network mainly covers the PAC, indicating a primary role in processing audio information. This feature is consistent with the audio cues used to prompt ankle movements for all tasks in this study. This network also covers some parts of the preSMA. When performing sequential movements, the preSMA participates in chunking and related processes, such as task switching, response selection, and response inhibition [42]. Thus, for sequential movements, such as simulated walking movements, preSMA can play a role in separating the motor task into minor fragments and in switching these fragments. The preSMA uses audio information from the PAC to achieve these functions. Other brain regions in these networks, including S2 and IPC, can provide sensory information for this

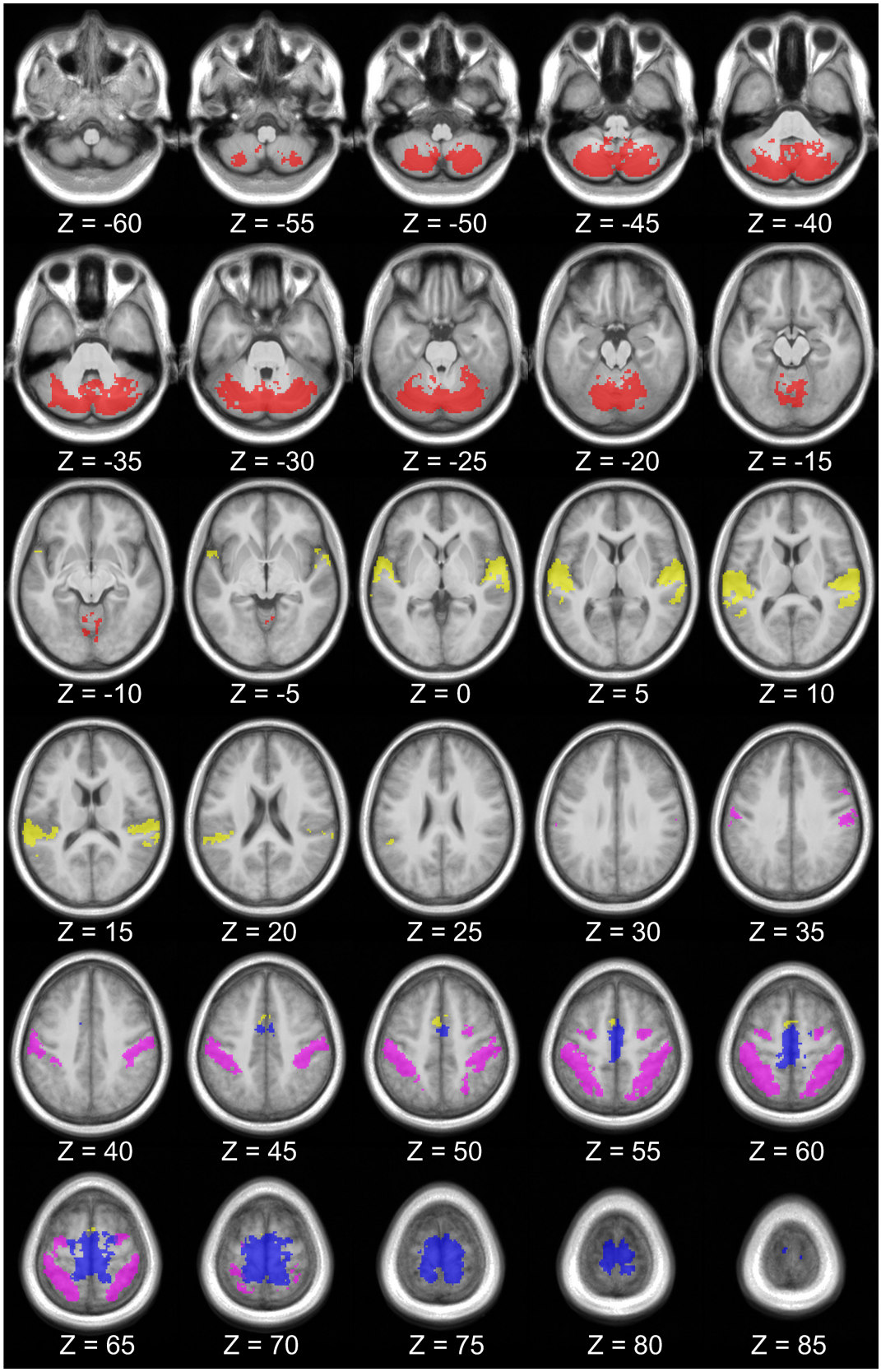

Fig. 1. Spatial maps of four independent components in all conditions. The spatial map of each commonly appearing independent component was projected on the average T1 images by using the MRIcron software (v1.0.20190902, https://www.nitrc.org/projects/mricron). The numbers indicate MNI coordinates in the *z*-axis. Cerebellum network: red; PAC-S2-IPC-preSMA network: yellow; medial M1S1-SMA-PreM-SPL network: blue; S1-SPL-PMd network: purple.

Table 1. Pairwise correlation values of different conditions.

0.5 Hz vs.1 Hz	0.75	0.69	0.65	0.63
	Cerebellum	PAC-S2-IPC-preSMA	Medial M1S1-SMA-PreM-SPL	lateral S1-SPL-PMd
0.5 Hz vs.2 Hz	0.75	0.68	0.65	0.63
	Cerebellum	Lateral S1-SPL-PMd	Medial M1S1-SMA-PreM-SPL	PAC-S2-IPC-preSMA
0.5 Hz vs. Changing-speed	0.74	0.65	0.62	0.59
	Cerebellum	Lateral S1-SPL-PMd	PAC-S2-IPC-preSMA	Medial M1S1-SMA-PreM-SPL
0.5 Hz vs. Free-speed	0.65	0.61	0.56	0.51
	Cerebellum	Lateral S1-SPL-PMd	Medial M1S1-SMA-PreM-SPL	PAC-S2-IPC-preSMA
0.5 Hz vs. Rest	0.71	0.59	0.55	0.35
	Cerebellum	Lateral S1-SPL-PMd	PAC-S2-IPC-preSMA	Medial M1S1-SMA-PreM-SPL
1 Hz vs.2 Hz	0.75	0.67	0.66	0.63
	Cerebellum	Lateral S1-SPL-PMd	Medial M1S1-SMA-PreM-SPL	PAC-S2-IPC-preSMA
1 Hz vs. Changing-speed	0.74	0.63	0.58	0.54
	Cerebellum	Lateral S1-SPL-PMd	PAC-S2-IPC-preSMA	Medial M1S1-SMA-PreM-SPL
1 Hz vs. Free-speed	0.65	0.60	0.53	0.52
	Cerebellum	Lateral S1-SPL-PMd	PAC-S2-IPC-preSMA	Medial M1S1-SMA-PreM-SPL
1 Hz vs. Rest	0.74	0.56	0.46	0.30
	Cerebellum	Lateral S1-SPL-PMd	PAC-S2-IPC-preSMA	Medial M1S1-SMA-PreM-SPL
2 Hz vs. Changing-speed	0.77	0.74	0.60	0.56
	Cerebellum	Lateral S1-SPL-PMd	PAC-S2-IPC-preSMA	Medial M1S1-SMA-PreM-SPL
2 Hz vs. Free-speed	0.68	0.66	0.57	0.57
	Cerebellum	Lateral S1-SPL-PMd	PAC-S2-IPC-preSMA	Medial M1S1-SMA-PreM-SPL
2Hz vs. Rest	0.70	0.54	0.44	0.36
	Cerebellum	Lateral S1-SPL-PMd	PAC-S2-IPC-preSMA	Medial M1S1-SMA-PreM-SPL
Changing-speed vs. Free-speed	0.68	0.66	0.58	0.57
	Cerebellum	Lateral S1-SPL-PMd	PAC-S2-IPC-preSMA	Medial M1S1-SMA-PreM-SPL
Changing-speed vs. Rest	0.68	0.57	0.57	0.33
	Cerebellum	Lateral S1-SPL-PMd	PAC-S2-IPC-preSMA	Medial M1S1-SMA-PreM-SPL
Free-speed vs. Rest	0.59	0.50	0.45	0.38
	Cerebellum	Lateral S1-SPL-PMd	PAC-S2-IPC-preSMA	Medial M1S1-SMA-PreM-SPL

function. The inferior temporal cortex preferentially participates in the cognitive aspects of discriminating shape and object, whereas the IPC plays roles in object-oriented action, object recognition, and motor planning [43]. This network controls the rhythm of the simulated walking tasks by integrating audio inputs (PAC), chunking/switching function (preSMA), and sensory processing in high-order sensory cortices (S2 and IPC).

4.3 Walking speed-differentiating network

The lateral S1-SPL-PMd network is mainly distributed in the parietal lobe, including the lateral parts of S1 and SPL. This network also covers a small part of PMd. This network presents a negative temporal correlation value with the time course of motor tasks with slow speeds (0.5 and 1 Hz) but a positive temporal correlation value with the time course of high-speed motor tasks (2 Hz, free- and changing-speed conditions). Thus, this network plays a role in differentiating walking speed.

The SPL participates in sensorimotor integration, such as tactile exploration [43] and processing kinesthetic cues during action-related somatosensory inputs [44]. The PMd controls proximal limb muscles for positioning the limb to perform a motor task during the preparation stage [45]. According to a previous study [46], the lateral part of S1 in this network covers the representation area of body parts above the knees but not the lower leg. We hypothesize that the lateral S1-SPL-PMd network integrates somatosensory inputs from the rest of the body (other than the moving part) and the functions of the PMd (movement preparation) and SPL (sensorimotor integration) to facilitate the involvement of the whole body during fast walking. This network does not directly control movement because M1 is not included in this network.

4.4 Basic actor network

The medial M1S1-SMA-PreM-SPL network is mainly distributed over the medial parts of M1 and S1 and covers the representation areas of the lower leg, including ankles and feet. These regions are commonly reported in previous fMRI studies on foot movements and are fundamental brain regions for motor execution and related sensory processing. Hence, this network is a basic actor network to control the walking movement.

This basic actor network can be detected in all motor task conditions and in the resting state. The map during the resting state covers more lateral parts of M1 and S1 than the map during task conditions (**Supplementary Fig.** 7). Such spa-

tial inconsistency leads to low correlation values (Table 1). The spatial map in the task conditions is only the medial part of the map in the resting state because only the lower leg is involved in motor tasks.

5. Conclusions

A rhythmic, bilaterally involved flexor-extensor alternating ankle movement was applied to simulate basic components of human walking on the basis of applied paradigms used in previous studies [1–3, 5, 7–12, 14, 47, 48]. Different speeds were used to provide variations. Four walking-control brain networks, namely, cerebellum, rhythm-control (PAC-S2-IPC-preSMA), walking speed-differentiating (lateral S1-SPL-PMd), and basic actor (medial M1S1-SMA-PreM-SPL) networks, were determined using ICA. These networks may be used as biomarkers of neural control of normal human walking and as targets for neural modulation to improve various aspects of walking, such as rhythm and speed.

The task paradigm in this study has not involved the body weight support, which is a basic factor during human walking in real situations. Therefore, the detected brain networks need to be confirmed by further studies investigating human walking in real contexts.

Abbreviations

BOLD, blood-oxygen-level-dependent; fMRI, functional magnetic resonance imaging; HRF, hemodynamic response function; IC, independent component; ICA, independent component analysis; IPC, inferior parietal cortex; M1, primary motor cortex; MDL, minimum description length; PAC, primary auditory cortex; PMd, dorsal premotor cortex; PMv, ventral premotor cortex; PreM, premotor cortex; S1, primary somatosensory cortex; S2, secondary somatosensory cortex; SMA, supplementary motor area; SPL, superior parietal lobule.

Author contributions

YF and PW conceived and designed the experiments; PW and TZ performed the experiments; PW analyzed the data; PW, TZ, ZL, and YF wrote the paper.

Ethics approval and consent to participate

Data were obtained with the informed consent of all participants. The institutional review board of the National Research Center for Rehabilitation Technical Aids approved the protocol, code 2018YFC2001401.

Acknowledgment

Not applicable.

Funding

This study was funded by the National Key R&D Program of China (Grant Nos. 2018YFC2001400 and 2018YFC2001700), the National Natural Science Foundation of China (Grant No. 81972160), and the Beijing Natural Science Foundation (Grant No. 17L20019).

Conflict of interest

The authors declare no conflict of interest.

Supplementary material

Supplementary material associated with this article can be found, in the online version, at https://doi.org/10.31083/j.jin2003074.

References

[1] Dobkin BH, Firestine A, West M, Saremi K, Woods R. Ankle dorsiflexion as an fMRI paradigm to assay motor control for walking during rehabilitation. NeuroImage. 2004; 23: 370–381.

[2] MacIntosh BJ, Mraz R, Baker N, Tam F, Staines WR, Graham SJ. Optimizing the experimental design for ankle dorsiflexion fMRI. NeuroImage. 2004; 22: 1619–1627.

[3] Sahyoun C, Floyer-Lea A, Johansen-Berg H, Matthews PM. Towards an understanding of gait control: brain activation during the anticipation, preparation and execution of foot movements. NeuroImage. 2004; 21: 568–575.

[4] Ciccarelli O, Toosy AT, Marsden JF, Wheeler-Kingshott CM, Sahyoun C, Matthews PM, *et al.* Identifying brain regions for integrative sensorimotor processing with ankle movements. Experimental Brain Research. 2005; 166: 31–42.

[5] Kapreli E, Athanasopoulos S, Papathanasiou M, Van Hecke P, Kelekis D, Peeters R, *et al.* Lower Limb Sensorimotor Network: Issues of Somatotopy and Overlap. Cortex. 2007; 43: 219–232.

[6] MacIntosh BJ, Baker SN, Mraz R, Ives JR, Martel AL, McIlroy WE, *et al.* Improving functional magnetic resonance imaging motor studies through simultaneous electromyography recordings. Human Brain Mapping. 2007; 28: 835–845.

[7] Enzinger C, Johansen-Berg H, Dawes H, Bogdanovic M, Collett J, Guy C, *et al.* Functional MRI Correlates of Lower Limb Function in Stroke Victims with Gait Impairment. Stroke. 2008; 39: 1507–1513.

[8] Huda S, Rodriguez R, Lastra L, Warren M, Lacourse MG, Cohen MJ, *et al.* Cortical activation during foot movements: II Effect of movement rate and side. NeuroReport. 2008; 19: 1573–1577.

[9] Newton JM, Dong Y, Hidler J, Plummer-D'Amato P, Marehbian J, Albistegui-Dubois RM, *et al.* Reliable assessment of lower limb motor representations with fMRI: use of a novel MR compatible device for real-time monitoring of ankle, knee and hip torques. NeuroImage. 2008; 43: 136–146.

[10] Francis S, Lin X, Aboushoushah S, White TP, Phillips M, Bowtell R, *et al.* FMRI analysis of active, passive and electrically stimulated ankle dorsiflexion. NeuroImage. 2009; 44: 469–479.

[11] Trinastic JP, Kautz SA, McGregor K, Gregory C, Bowden M, Benjamin MB, *et al.* An fMRI study of the differences in brain activity during active ankle dorsiflexion and plantarflexion. Brain Imaging and Behavior. 2010; 4: 121–131.

[12] Cauda F. MR compatible device for active and passive foot movements. International Journal of Mechanics and Control. 11,2010; 11: 29–38.

[13] Jaeger L, Marchal-Crespo L, Wolf P, Riener R, Michels L, Kollias S. Brain activation associated with active and passive lower limb stepping. Frontiers in Human Neuroscience. 2014; 8: 828.

[14] Hotz-Boendermaker S, Funk M, Summers P, Brugger P, Hepp-Reymond M, Curt A, *et al.* Preservation of motor programs in paraplegics as demonstrated by attempted and imagined foot movements. NeuroImage. 2008; 39: 383–394.

[15] Jahn K, Deutschländer A, Stephan T, Kalla R, Wiesmann M, Strupp M, *et al.* Imaging human supraspinal locomotor centers in brainstem and cerebellum. NeuroImage. 2008; 39: 786–792.

[16] Wang C, Wai Y, Kuo B, Yeh Y, Wang J. Cortical control of gait in healthy humans: an fMRI study. Journal of Neural Transmission. 2008; 115: 1149–1158.
[17] La Fougère C, Zwergal A, Rominger A, Förster S, Fesl G, Dieterich M, *et al.* Real versus imagined locomotion: a [18F]-FDG PET-fMRI comparison. NeuroImage. 2010; 50: 1589–1598.
[18] Sacheli LM, Zapparoli L, De Santis C, Preti M, Pelosi C, Ursino N, *et al.* Mental steps: Differential activation of internal pacemakers in motor imagery and in mental imitation of gait. Human Brain Mapping. 2017; 38: 5195–5216.
[19] Minassian K, Hofstoetter US, Dzeladini F, Guertin PA, Ijspeert A. The Human Central Pattern Generator for Locomotion: does it Exist and Contribute to Walking? The Neuroscientist. 2017; 23: 649–663.
[20] Radhakrishna M, Steuer I, Prince F, Roberts M, Mongeon D, Kia M, *et al.* Double-Blind, Placebo-Controlled, Randomized Phase i/IIa Study (Safety and Efficacy) with Buspirone/Levodopa/Carbidopa (SpinalonTM) in Subjects with Complete AIS a or Motor-Complete AIS B Spinal Cord Injury. Current Pharmaceutical Design. 2017; 23: 1789–1804.
[21] Paret C, Kluetsch R, Ruf M, Demirakca T, Kalisch R, Schmahl C, *et al.* Transient and sustained BOLD signal time courses affect the detection of emotion-related brain activation in fMRI. NeuroImage. 2015; 103: 522–532.
[22] Contreras-Vidal JL, Kerick SE. Independent component analysis of dynamic brain responses during visuomotor adaptation. NeuroImage. 2004; 21: 936–945.
[23] Pruim RHR, Mennes M, van Rooij D, Llera A, Buitelaar JK, Beckmann CF. ICA-AROMA: a robust ICA-based strategy for removing motion artifacts from fMRI data. NeuroImage. 2015; 112: 267–277.
[24] James GA, Hazaroglu O, Bush KA. A human brain atlas derived via n-cut parcellation of resting-state and task-based fMRI data. Magnetic Resonance Imaging. 2016; 34: 209–218.
[25] Rzucidlo JK, Roseman PL, Laurienti PJ, Dagenbach D. Stability of whole brain and regional network topology within and between resting and cognitive states. PLoS ONE. 2013; 8: e70275.
[26] Wei P, Zou T, Lv Z, Fan Y. Functional MRI Reveals Locomotion-Control Neural Circuits in Human Brainstem. Brain Sciences. 2020; 10: 757.
[27] Napadow V, Dhond R, Kennedy D, Hui KKS, Makris N. Automated brainstem co-registration (ABC) for MRI. NeuroImage. 2006; 32: 1113–1119.
[28] Rissanen J. A Universal Prior for Integers and Estimation by Minimum Description Length. The Annals of Statistics. 1983; 11: 416–431.
[29] Bell AJ, Sejnowski TJ. An information-maximization approach to blind separation and blind deconvolution. Neural Computation. 1995; 7: 1129–1159.
[30] Himberg J, Hyvärinen A, Esposito F. Validating the independent components of neuroimaging time series via clustering and visualization. NeuroImage. 2004; 22: 1214–1222.
[31] Calhoun VD, Adali T, Pearlson GD, Pekar JJ. A method for making group inferences from functional MRI data using independent component analysis. Human Brain Mapping. 2001; 14: 140–151.
[32] McKeown MJ, Hansen LK, Sejnowsk TJ. Independent component analysis of functional MRI: what is signal and what is noise? Current Opinion in Neurobiology. 2003; 13: 620–629.
[33] De Luca M, Smith S, De Stefano N, Federico A, Matthews PM. Blood oxygenation level dependent contrast resting state networks are relevant to functional activity in the neocortical sensorimotor system. Experimental Brain Research. 2005; 167: 587–594.
[34] Brooks JCW, Beckmann CF, Miller KL, Wise RG, Porro CA, Tracey I, *et al.* Physiological noise modelling for spinal functional magnetic resonance imaging studies. NeuroImage. 2008; 39: 680–692.
[35] Beissner F, Schumann A, Brunn F, Eisenträger D, Bär K. Advances in functional magnetic resonance imaging of the human brainstem. NeuroImage. 2014; 86: 91–98.
[36] Morosan P, Rademacher J, Schleicher A, Amunts K, Schormann T, Zilles K. Human primary auditory cortex: cytoarchitectonic subdivisions and mapping into a spatial reference system. NeuroImage. 2001; 13: 684–701.
[37] Bailey L, Abolmaesumi P, Tam J, Morosan P, Cusack R, Amunts K, *et al.* Customised cytoarchitectonic probability maps using deformable registration: primary auditory cortex. International Conference on Medical Image Computing and Computer-Assisted Intervention (pp. 760–768). Springer: Berlin. 2007.
[38] Mayka MA, Corcos DM, Leurgans SE, Vaillancourt DE. Three-dimensional locations and boundaries of motor and premotor cortices as defined by functional brain imaging: a meta-analysis. NeuroImage. 2006; 31: 1453–1474.
[39] Ramachandran VS. Encyclopedia of the Human Brain (Volume 4). 1st edn. Academic Press: San Diego. 2002.
[40] Standring S. Gray's Anatomy. 39th edn. Churchill Livingstone: UK. 2004.
[41] Allan HR, Brown RH. Adams and Victor's Principles of Neurology. 8th edn. McGraw-Hill: New York. 2005.
[42] Xu B, Sandrini M, Wang W, Smith JF, Sarlls JE, Awosika O, *et al.* PreSMA stimulation changes task-free functional connectivity in the fronto-basal-ganglia that correlates with response inhibition efficiency. Human Brain Mapping. 2016; 37: 3236–3249.
[43] Jäncke L, Kleinschmidt A, Mirzazade S, Shah NJ, Freund HJ. The role of the inferior parietal cortex in linking the tactile perception and manual construction of object shapes. Cerebral Cortex. 2001; 11: 114–121.
[44] Hartmann S, Missimer JH, Stoeckel C, Abela E, Shah J, Seitz RJ, *et al.* Functional connectivity in tactile object discrimination: a principal component analysis of an event related fMRI-Study. PLoS ONE. 2008; 3: e3831.
[45] Haines DE, Mihailoff GA. Fundamental Neuroscience for Basic and Clinical Applications. 5th end. Elsevier Health Sciences: Philadelphia. 2018.
[46] Bao R, Wei P, Li K, Lu J, Zhao C, Wang Y, *et al.* Within-limb somatotopic organization in human SI and parietal operculum for the leg: an fMRI study. Brain Research. 2012; 1445: 30–39.
[47] Christensen MS, Lundbye-Jensen J, Petersen N, Geertsen SS, Paulson OB, Nielsen JB. Watching your foot move-an fMRI study of visuomotor interactions during foot movement. Cerebral Cortex. 2007; 17: 1906–1917.
[48] Orr ELR, Lacourse MG, Cohen MJ, Cramer SC. Cortical activation during executed, imagined, and observed foot movements. NeuroReport. 2008; 19: 625–630.